Comparison of Steel and Reinforced Concrete Frames' Durability under Fire and Post-Earthquake Fire Scenario

Moradi, M.[1], Tavakoli, H.R.[2]* and Abdollahzadeh, Gh.[3]

[1] Ph.D. Student, Faculty of Civil Engineering, Babol Noshirvani University of Technology, Babol, Iran.
[2] Associate Professor, Faculty of Civil Engineering, Babol Noshirvani University of Technology, Babol, Iran.
[3] Professor, Faculty of Civil Engineering, Babol Noshirvani University of Technology, Babol, Iran.

© University of Tehran 2021

ABSTRACT: Two fire accidents took place in the Plasco Tower in Iran and Grenfell Tower of London in 2017. Although both of them have led to human tragedies, post-earthquake fire can cause more irreparable damages and catastrophes in larger extents. Engineering structures are subjected to different loads during their lifetime, which may cause damage or secondary loading effects. Evaluation of durability and stability of fired structures and the effects of seismic loading are considered to be significant parameters in fire engineering. The aim of this study is to evaluate and compare durability of reinforced concrete and steel frames during fire loading and post-earthquake fires. In this study, two 7-story steel and reinforced concrete frames are exposed to the fire load. At first, steel and concrete sections are put under various thermal loads in order to compare the method of their heat transfer. Then, the effects of crack on heat transfer of concrete sections are studied. Afterwards, the selected frames are exposed to the fire and post-earthquake fires. The results indicated that cracking and strength reduction due to seismic loading can decrease the durability of reinforced concrete frame in post-earthquake fire scenarios. However, the durability of steel frames has no significant relationship with the seismic loading and their durability are almost the same in the fire and post-earthquake fire scenarios.

Keywords: Failure Time, Heat Transfer, Post-Earthquake Fire, Reinforced Concrete Frame, Steel Frame.

1. Introduction

Different types of loads threaten the structural strength of buildings. Earthquake, fire, explosion, etc. are those kinds of hazards which can jeopardize structural strength (Moradi et al., 2019). Each load creates a different response in structures. The most significant load, which can put at risk the strength of structures in designs, is seismic load (Moradi et al., 2019). However, a few loads result in large and noticeable responses in the structure. Earthquake reduces the strength of

structures against further loads. In addition to the damages which are caused by earthquake itself, it has some subsequent consequences. These consequences in nature are landslide and tsunami. Moreover, earthquake itself cause some dangers for structures (Tavakoli and Moradi, 2018). Earthquake damages to electrical and gas transmission lines lead to fire and its spreading to the adjacent stories creates a fire catastrophe.

Many countries, such as Japan, have experienced post-earthquake fire several times. Fire and Post-Earthquake Fire (PEF) are considered to be a serious threat for human societies. This is a rare event with a lot of probable consequences (Nishino et al., 2012). PEF is a real threat in high density places. This kind of fire has been known as a destructive and severe force in the last century (Lee and Davidson 2010).

The strength of structures against natural disasters, such as PEF, is reducing rapidly. Many structures have been damaged by PEF. Different structural elements lose their strength and stability on exposure to high temperatures (Shachar et al., 2020). This reduction in strength will increase if the elements are damaged by seismic loads (Memari et al. 2014).

The evaluation of the response of structures under multi-hazard scenarios has been developed in recent years. Song et al. (2010) analyzed post-fire cyclic behaviors of reinforced concrete bearing walls. Sharma et al. (2012) have put some experimental samples of damaged reinforced concrete frame under thermal loadings. Kadir et al. (2012) surveyed PEF scenarios by some limited two dimensional (2D) and three dimensional (3D) limited models. Zolfaghari et al. (2009) tried to provide an analytical approach to model sources of intra-structure ignitions and their associated uncertainties.

Keller and Pessiki (2015) described damage patterns in Sprayed Fire Resistive Material (SFRM) in a steel moment frame beam-column assemblages owing to a strong seismic event, and the thermal consequences of this damage when it is exposed to PEF. Memari et al. (2014) utilize Finite Element simulations to provide insight into the effects of earthquake initiated fires on low-, medium-, and high-rise steel moment resisting frames' connections with reduced beam sections that have become common in modern earthquake-resistant design since the Northridge earthquake of 1994.

Keller and Pessiki (2012) presented an analytical case study designed to evaluate the effect of experimental observed SFRM spall patterns on the thermo-mechanical response of a steel moment frame beam-column assembly during PEF. Many examples of PEF are recorded in the history. In 1971, San Fernando earthquake created 116 PEF's. In 1989, Loma-Prieta earthquake created 110 PEF's, 86% of which occurred in building structures. In 1995, Kobe earthquake created 108 PEF's, 97% of which occurred in building structures. In 2004, Niigata earthquake created 9 catastrophes due to PEF (Elhami Khorasani and Garlock, 2017).

Many experimentally and numerically researches are carried out separately on evaluation of steel and concrete structures' behavior in fire and PEF scenarios (Tavakoli and Kiakojuri, 2015). Despite the notable number of studies investigating post-earthquake fire scenarios, there is a significant gap in the comparison of structural behavior during fire and PEF scenarios. This study aims to analyze and compare the response and durability of RC and steel frames against post-earthquake fire loading.

To this end, steel and concrete sections are exposed to different thermal loads in order to analyze heat transfer procedure in these sections. Since RC sections may be cracked and spalling under seismic loads (Barkavi and Natarajan, 2019), they are analyzed according to their cracking effects with different widths and depths of the crack in order to estimate their effect on heat transfer analysis. After heat transfer analysis of the sections, two 7-story steel

and reinforced moment resisting frames are put under nonlinear analysis by their modeled mechanical-thermal properties and their behaviors against thermal loads are surveyed under thermal load alone.

In this section, the time of durability are considered as analysis parameters during different fire load scenarios. According to analysis parameters, a dynamic evaluation is carried out on strength and performance levels of the structures under various seismic loads. Consequently, based on the cracking effects and strength reduction in reinforced concrete structures, durability of reinforced concrete and steel frames in PEF loadings are estimated.

2. Methodology

2.1. Structural Models

As mentioned in section 1, two dimensional (2D) 7-story RC and steel Moment Resisting Frames (MRF) were used for PEF analyzing. At first, a three dimensional (3D) structure with a square plan (4@4 m) was modeled and designed (Figure 1). Height of each story was assumed to be 3 meters.

For structural design, dead load is

considered to be 600 kg/m^2, live load is 200 kg/m^2, and equivalent snow load is 150 kg/m^2. According to Iranian seismic code, a high seismic area with PGA of 0.35 g and type III soil was used for applying lateral load. Iranian seismic and design guidelines were used for structural loading and designs.

Steel yield strength is 240 MPa, and Young's modulus of steel material is 2e5 Mpa. Ultimate strength of concrete (f_c) is 21 MPa, strength of rebars is 338 MPa, Poisson ratio for steel is 0.3, and for concrete materials is 0.2. After design, the middle frame span (Frame C in Figure 1) was selected from the structures. The results of designs, which are done based on the structural sections, are indicated in Table 1:

2.2. Heat Transfer

Density, thermal conductivity, and specific heat are the main parameters in various materials. In exposure to fire, heat transfer starts from the most external sections and moves toward colder and farther sections. According to the references (Wong and Ghojel, 2003), thermal gradient is representable based on Eq. (1):

Table 1. Steel structural sections

| Steel frame						
Story	Beam				Column	
	Web height	Web thickness	Flange width	Flange thickness	H	t
1	45	0.78	17	1.3	45	2
2	45	0.78	17	1.3	45	2
3	40	0.68	17	0.97	40	2
4	40	0.68	17	0.97	40	2
5	30	0.6	14.6	0.9	30	1.2
6	30	0.6	14.6	0.9	30	1
7	25	0.5	12	0.8	20	1
RC frame						
Story	H	Bottom rebar	Top rebar	H	Rebar	
1	45	8 d20	7 d20	70	20 d22	
2	45	8 d20	7 d20	70	20 d22	
3	45	8 d16	6 d16	60	18 d20	
4	40	7 d 16	6 d16	50	20 d18	
5	35	7 d 12	6 d 12	50	20 d18	
6	35	7 d 12	5 d 12	35	18 d16	
7	35	5 d 12	4 d 12	35	18 d16	
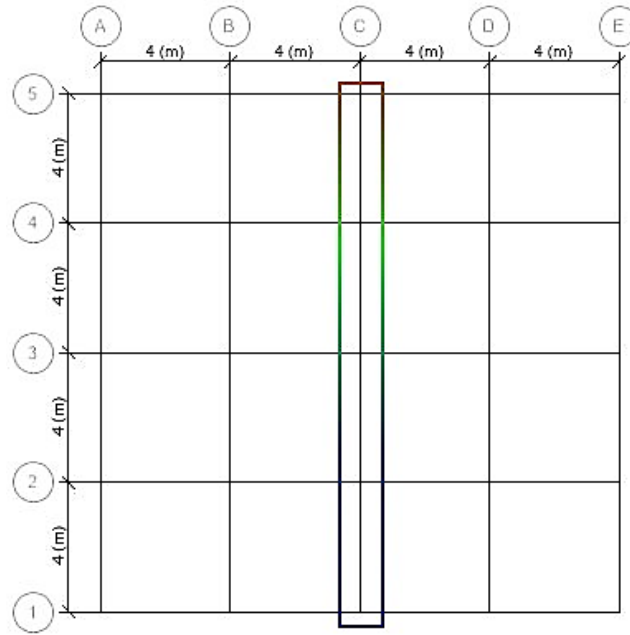
Fig. 1. Plans of the selected structures

$$(\rho_w c_w + \rho_c c_c + \rho_l c_l)\frac{\partial T}{\partial t}$$
$$= \frac{\partial}{\partial x}\left[\lambda_x \frac{\partial T}{\partial x}\right]$$
$$+ \frac{\partial}{\partial y}\left[\lambda_y \frac{\partial T}{\partial y}\right] \qquad (1)$$
$$+ \frac{\partial}{\partial z}\left[\lambda_z \frac{\partial T}{\partial z}\right] + Q_r^{"}$$

where T: stands for temperature, λ: for thermal conductivity, ρ: for material density and C: for specific heat. $Q_r^{"}$: is the sum of reaction heat of the different pyrolysis reactions at the temperature T. Moreover, x, y, and z: are three coordinate directions.

Thermal conductivity and specific heat parameters were considered as a temperature function. A material's thermal conductivity is the number of Watts conducted per meter thickness of the material, per degree of temperature difference between one side and the other side (W/mK). Specific heat capacity is defined as the amount of heat required to raise the temperature of 1 Kg of a substance by 1 Kelvin (SI unit of specific heat capacity J/Kg.K)

Different values of thermal conductivity and specific heat of steel and concrete materials are indicated in Figures 2 and 3. Density was selected to be 7.85 g/cm^3 for steel materials, and 2.4 g/cm^3 for concrete

materials (Natesh and Agarwal, 2020). In order to heat transfer analysis, all structural sections were modeled by ABAQUS these parameters is shown in Table 1. Although Opensees performs heat transfer analysis, for greater accuracy, Abaqus software is used to heat transfer analysis. Then, thermal conductivity, density, and specific heat parameters were modeled in the same software and analyzed after defining fire load of heat transfer in different sections.

2.3. Mechanical-Thermal Analysis

For PEF analysis, an accurate mechanical-thermal model of the frame is needed. OpenSees was used to do thermal modeling. Mechanical parameters of RC materials have different behaviors toward heat (Eskandari et al., 2013). The modulus of elasticity, strain, and strength of materials were mechanical properties which vary with change of temperatures. Elasticity modulus and strength of concrete and steel will decrease by temperature rising. However, this change, unlike elasticity modulus and strength, is followed by a significant increase. Studied the behavior of concrete and steel materials as the temperature rises. Figure 4 represents the changes of concrete and steel strength according to temperature rise.
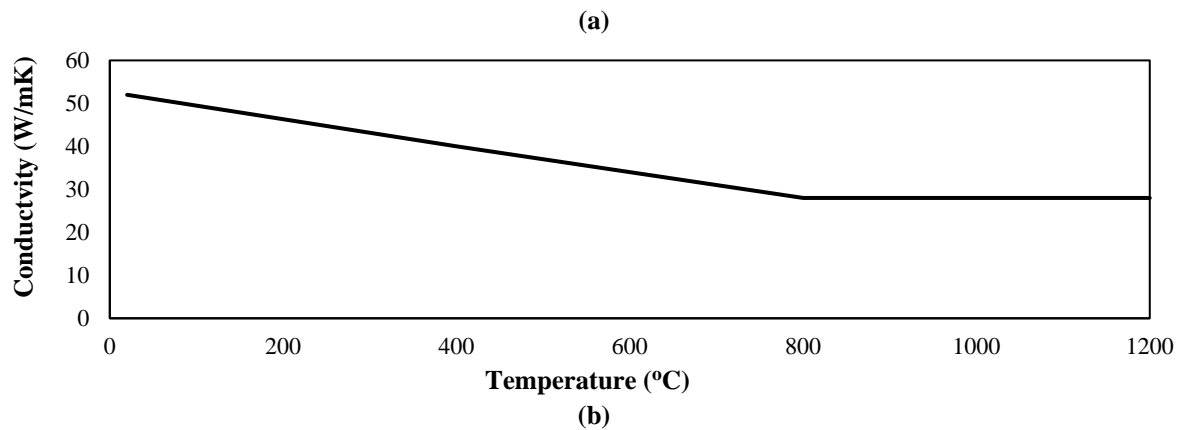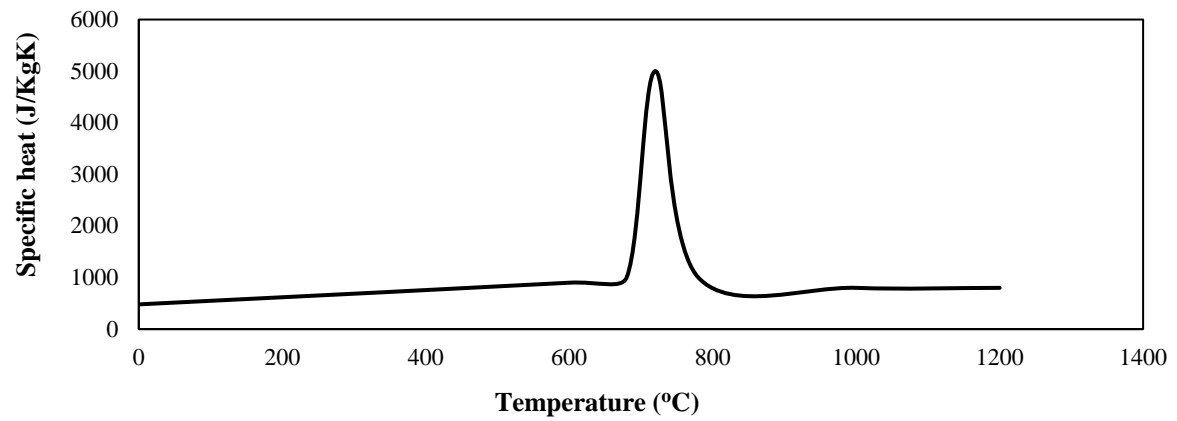
Fig. 2. Ratio of thermal properties changes in steel materials to temperature rise: a) Specific heat and; b) thermal conductivity coefficient (Tavakoli and Moradi, 2018)
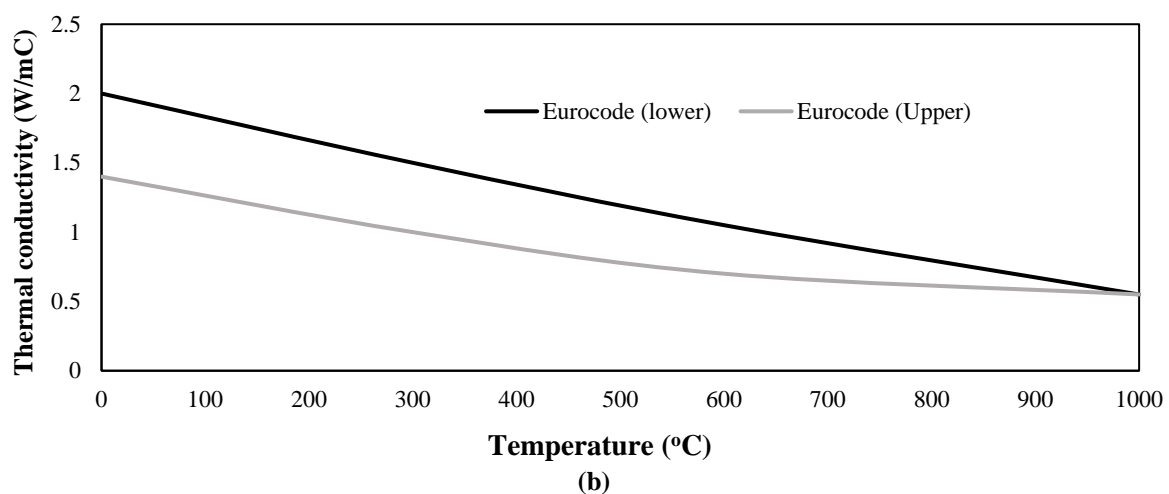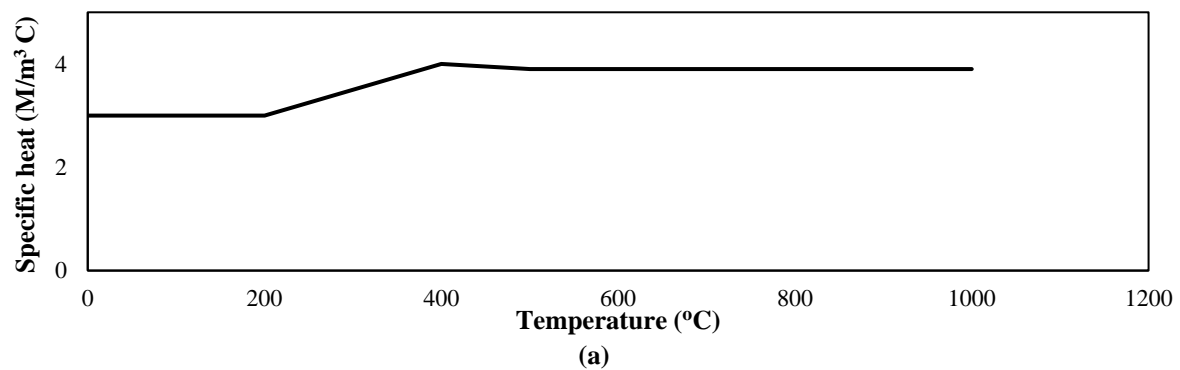

Fig. 3. Ratio of thermal properties changes in concrete materials to temperature rise: a) Specific heat and; b) thermal conductivity coefficient (Moradi et al., 2019)
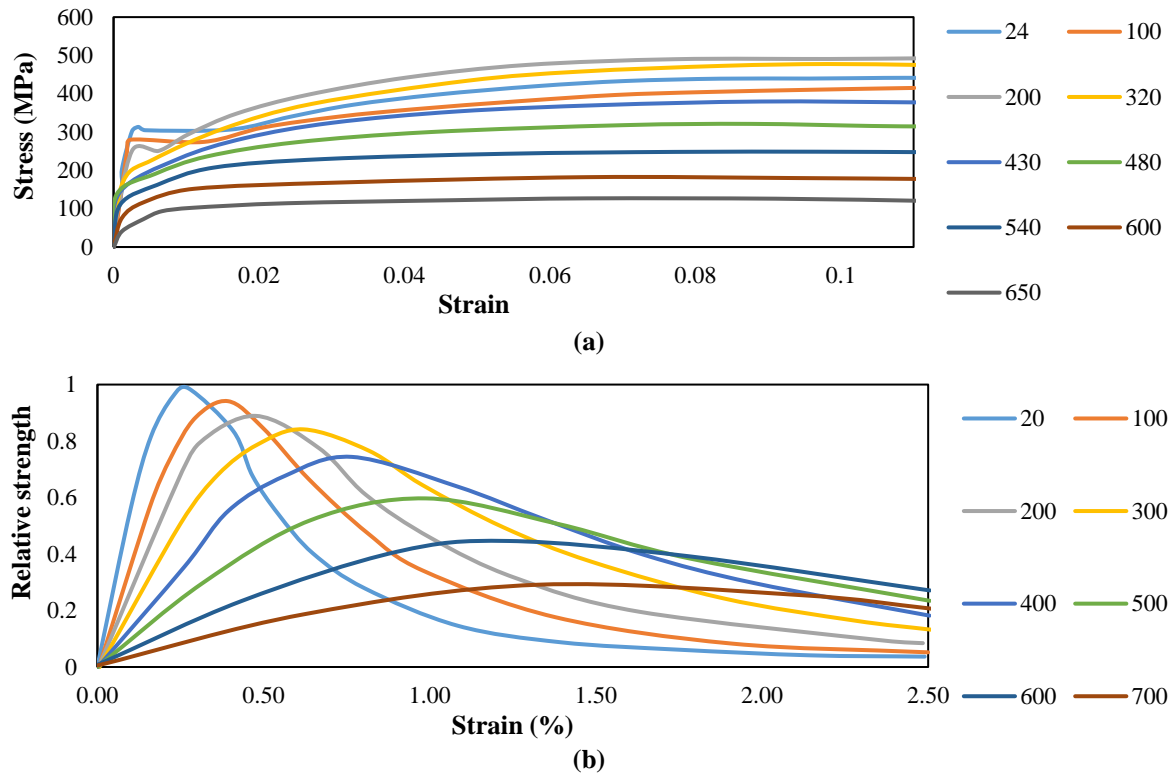
Fig. 4. A sample curve for properties changes of materials according to temperature rise: a) Strength of steel materials and; b) bearing strength of concrete materials (Felicetti et al., 1996)

In this study, the effect of cracking and spalling caused by a seismic load on heat transfer analysis in reinforced concrete sections is considered. In any seismic intensity, the damage index has been used to determine cracking and spalling. The effect of the cracks in the heat transfer analysis has been applied in the areas of the plastic hinges.

OpenSees is an open source software which was used for structural and earthquake engineering analysis. This software is basically designed for nonlinear analysis of structures. It is used by Edinburgh University for thermal and fire loading analysis. In fact, this software has the capability of doing thermal and mechanical-thermal analysis (Usmani et al., 2012). In this software, steel thermal materials are Steel01thermal and steel02thermal type; thermal materials of concrete are from Concrete02thermal type which are presented based on EN 1992-1-2 standards. Ratio of the decrease in different parameters to temperature rise is indicated in Table 2. In this table, $f_{sp,\theta}$: is the strength of steel in the fit limit for the specified

temperature, $f_{sy,\theta}$: is the yield strength of steel in the specified temperature, f_{yk}: is the yield strength in 20 ℃, $E_{s,\theta}$: is elasticity modulus of steel in the specified temperature, $\varepsilon_{cu\theta}$: is the final concrete strain in the specified temperature, $\varepsilon_{c\theta}$: is the strain of concrete in the maximum compressive strength and $f_{c,\theta}$: is the maximum compressive strength of concrete.

In this study, two dimensional (2D) models were used for mechanical-thermal analysis. Therefore, all the selected frames were modeled two dimensionally and their mechanical-thermal loadings, deformations, and created forces were analyzed (Kotsovinos and Usmani, 2013). This study indicated that two dimensional models in OpenSees can accurately estimate the created horizontal displacements due to thermal loadings. For thermal modeling, DispBeamColumnThermal element, Concrete02thermal, and steel02thermal materials were used to model concrete and steel materials. In Figure 5, modeling of elements with mechanical and thermal properties are indicated schematically by

OpenSees software.

The seismic and thermal analysis in the frame was applied continuously. So the residual strain effects due to the seismic loading has been automatically considered in thermal loading.

2.4. Thermal Loading

As mentioned in section 1, the purpose of this study is to analyze and compare the durability of steel and RC moment frames in fire, and PEF scenarios. Therefore, at first, a thermal analysis should be carry out under fire load. For thermal analysis, it was assumed that fire is caused by gas combustion in a closed area. Structural vulnerability against heat is dependent on temperature rise in the area. Growth rate of fire, released heat rate, and fire load are three main factors which affect the estimation of fire properties. For thermal analysis in an area, many factors are significant, such as fuel, geometry of the area, openings, etc. Generally, fire load is used for analyzing temperature rise of a closed area. Many studies have been done on the effects of different parameters on the fire load. Also, many researchers conducted different researches on the analysis of fire load and the resulted temperature-time curve. In this study, temperature-time curves were used for 100, 300, 500, 600, 700, 900, and 1000 fire loads in addition to ISO 834 standard thermal load. Therefore, 8 temperature-time curves are used for thermal loads. These curves are indicated in Figure 6.

Table 3 represents the maximum corresponding temperature of each fire load. All the thermal analysis lasted 2 hours. For thermal load modeling in OpenSees software, temperature-time curves of each section should be applied on elements. For estimation of temperature-time curves in the depth of each section, each of them are applied on sections according to the corresponding fire load. Consequently, after heat transfer analysis, temperature-time curves in the depth of each section are used in OpenSees software.

**Table 2.** Changes of concrete and steel material parameters according to different temperatures

Concrete02thermal			
$\theta(^{o}c)$	$f_{c,\theta}/f_{ck}$	$\varepsilon_{c\theta}$	$\varepsilon_{cu\theta}$
20	1	0.0025	0.02
100	1	0.004	0.0225
200	0.95	0.0055	0.025
300	0.85	0.007	0.0275
400	0.75	0.01	0.03
500	0.6	0.015	0.0325
600	0.45	0.025	0.035
700	0.3	0.025	0.0375
800	0.15	0.025	0.04
900	0.08	0.025	0.0425
1000	0.04	0.025	0.045
1100	0.01	0.025	0.0475

Steel02thermal		
$F_{sy,\theta}/f_{yk}$	$F_{sp,\theta}/f_{yk}$	$E_{s,\theta}/E_s$
1	1	1
1	0.96	1
1	0.92	0.87
1	0.81	0.72
0.94	0.63	0.56
0.67	0.44	0.4
0.4	0.26	0.24
0.12	0.08	0.08
0.11	0.06	0.06
0.08	0.05	0.05
0.05	0.03	0.03
0.03	0.02	0.02

Table 3. The specified fire load and maximum resulted temperature because of each fire load (Khorasani et al., 2014)

Name	Q100	Q300	Q500	Q600
Q (MJ/m^3)	100	300	500	600
T (C)	781	934	1011	1038
Name	Q700	Q900	Q1000	ISO
Q (MJ/m^3)	700	900	1000	834
T (^{o}C)	1061	1098	1113	1050
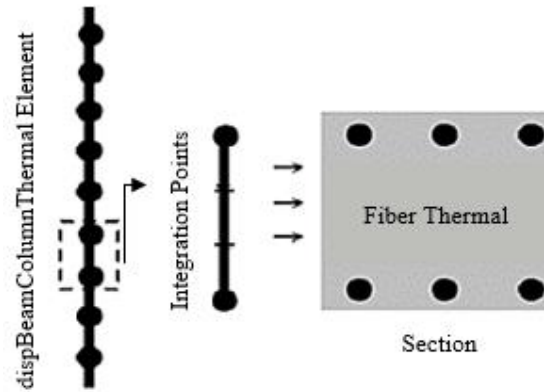
Fig. 5. Schematic figure of mechanical and thermal elements modeling in OpenSees
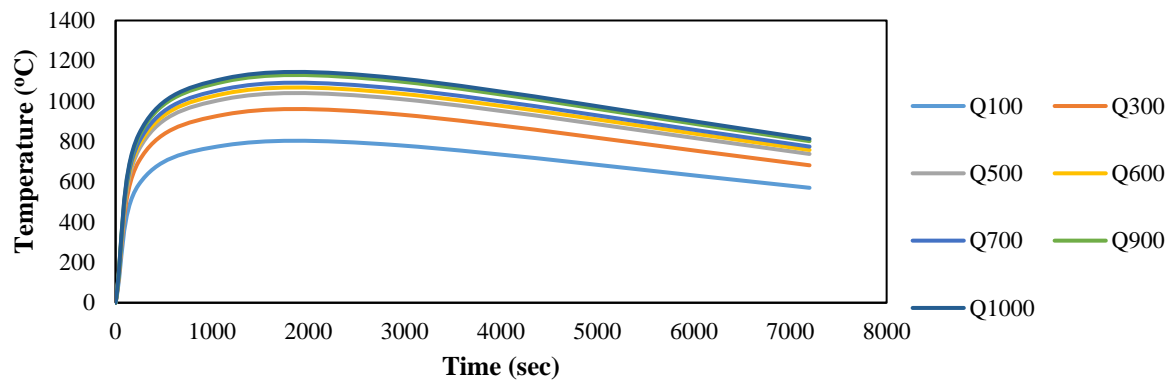
(a)
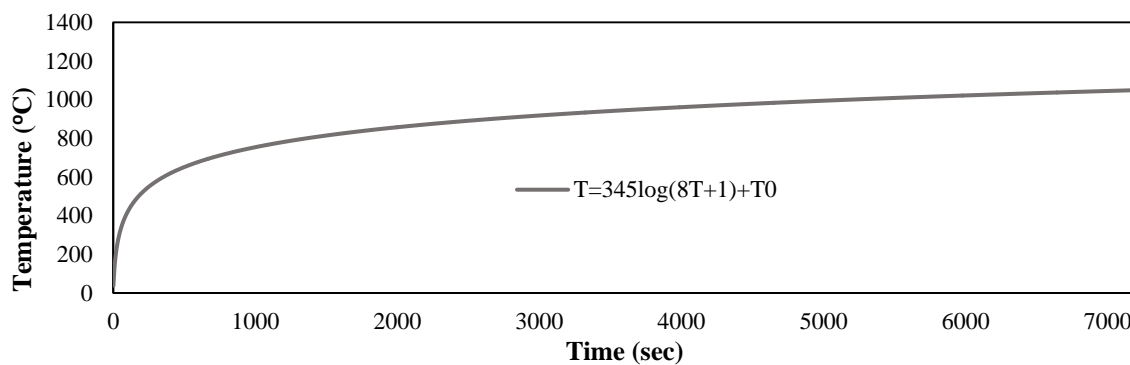
(b)

Fig. 6. Temperature-time curve: a) natural fire load and; b) ISO 834

2.5. Seismic Load

In this study, ten records of earthquake were used for nonlinear seismic analysis. According to the statistics, the earthquakes of Niigata (1964), San Fernando (1971), Loma Prieta (1989), Northridge (1994), and Kobe (1995) caused fire in the structure and PEF in which inability of firefighters and transmission of fire to adjacent structures caused human disasters (Tan et al., 2020).

The above mentioned earthquakes, which created PEF, and 5 other earthquakes were selected for this study (Table 4). The stations which are located in ground type III were used for selecting records. Each of the earthquakes were scaled based on Iranian 2800 standard and applied to the structures. To model the scale of earthquakes, at first all of the records were scaled on 1g. Then, response spectrum was extracted according to 5% damping. After that, the mean of response spectrum were scaled based on the design spectrum of Iranian seismic code. Figure 7 indicated each response spectrum and the spectrum of standard design.

2.6. Loading Scenarios

As mentioned before, eight patterns of fire loads and 10 ones of seismic loads are used in this study. Seismic and thermal loads are applied on 7-story frames including steel and RC frames after mechanical-thermal modeling. In this study, three locations were selected for fire area. Thermal loads were applied on each of them after earthquake. Fire area in this study was limited to a middle span at the first, third, and sixth story. Initially, thermal load is applied on each of the spans. After identifying the behavior of frames under fire load, seismic analysis were performed in order to estimate the effects of seismic loads. After studying the structural behavior under fire and seismic loads, frames were placed in the specified spans; then, thermal and seismic loads were applied on them. In this section of the study, each of the structures were put under seismic loads. Immediately after finishing seismic load, fire load was applied on them. Each of the steel and RC frames were exposed to the PEF fire scenarios by ten seismic loads. Each seismic load was followed by 8 patterns of fire loads in itself. Therefore, steel and RC frames were exposed to 80 PEF loadings. By considering three separate locations, totally 240 mechanical-thermal loadings were applied on each frame. The time of a sudden increase in the vertical displacement of the middle span of the beam was considered as the failure criterion of the structure under PEF loads. Figure 8 indicates a schematic for PEF scenario.

Table 4. The characteristic of earthquake

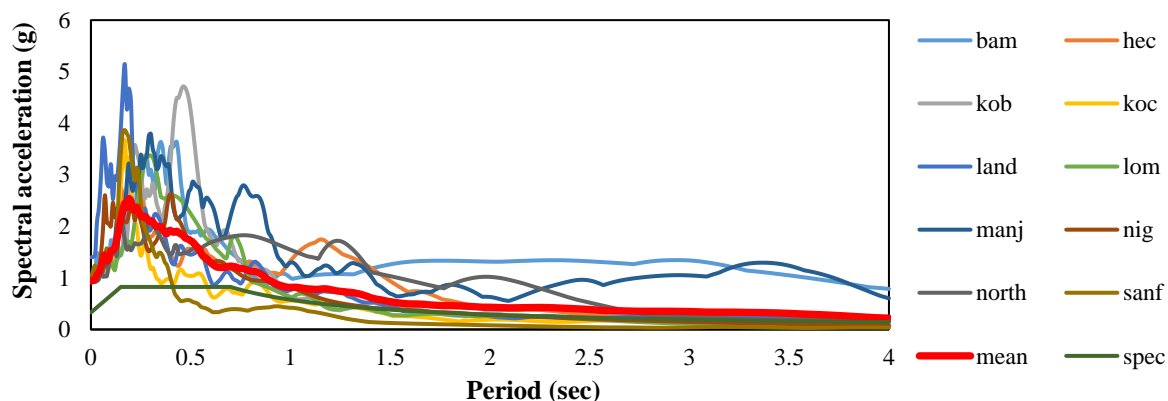| Event	Year	Station	Mag.	PGA (g)
Niigata	2004	NIGH11	6.63	0.59
Kobe	1995	Nishi-Akashi	6.9	0.48
Loma Prieta	1989	Corralitos	6.93	0.645
Northridge	1994	LA Dam	6.69	0.426
San Fernado	1971	Lake Hughes #12	6.61	0.38
Bam	2003	Bam	6.6	0.807
Hector Mine	1999	Hector	7.13	0.265
Kocaeli	1999	Arcelik	7.51	0.21
Landers	1992	Yermo Fire st	7.28	0.15
Manjil	1990	Abhar	7.37	0.13

Fig. 7. Response spectrum of records

2.7. Verification

The experimental researches which have been done on PEF's in reinforced concrete structures have no sufficient accuracy (Moradi et al. 2019). In this study, the experimental model of Imani et al. (2014) was used to verify the process. They exposed a ductile concrete-filled double-skin tube column to cyclic loads in the form of load control. Then, they exposed it to fire loads and estimated its deformation and durability. The lateral load Pattern of Imani experimental model is indicated in Figure 9.

Steel02Thermal and Concrete02Thermal were used as reinforced concrete and steel materials which form this column. Moreover, for the modeling of sections, mechanical-thermal fibers were used. For mechanical-thermal models, dispBeamcolumnThermal element was used. The column was modeled and loaded

based on Imani et al. (2014) experimental model. The results of cyclic analysis of this column which was exposed to lateral load (Figure 9), is indicated in Figure 10a. The results of nonlinear mechanical analysis show that the result of numerical modeling in this study has acceptable correspondence with Imani et al. (2014). Modeled samples were put under mechanical and thermal analysis, respectively. Fire loads wre applied based on Imani et al. (2014) temperature-time curves. Vertical displacement curve of column was extracted and showed based on time as an analysis parameter (Figure 10b). In this study, two gauges were located in northern and southern sections. Then, their vertical deformations were analyzed. The results indicated that the failure time has a sufficient agreement with Imani et al. (2014) experimental model.
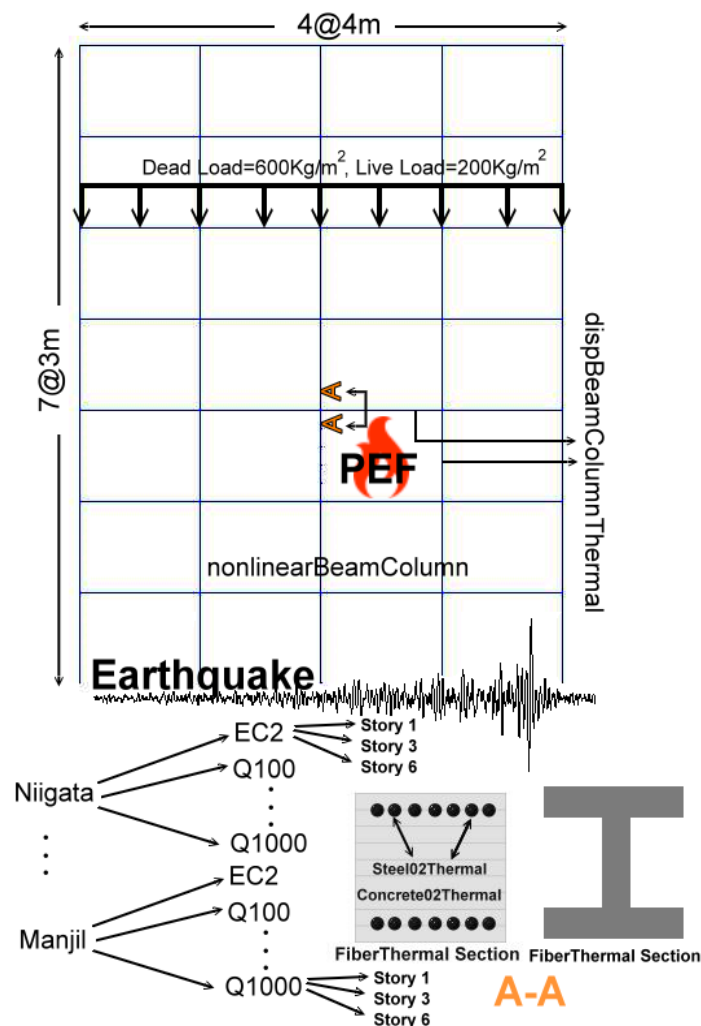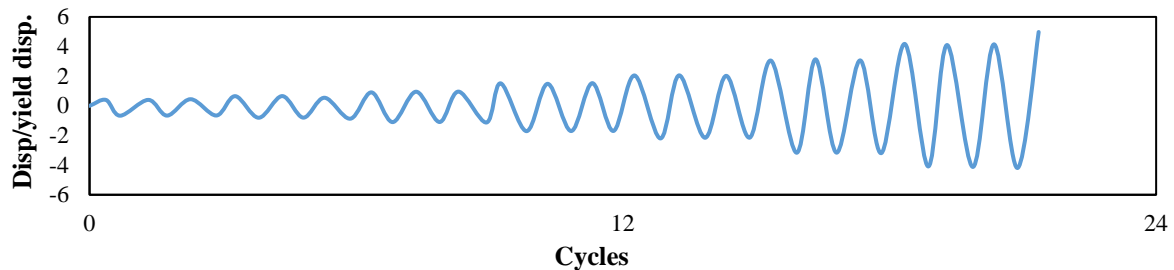

Fig. 8. Schematic of PEF scenario

Fig. 9. Imani et al. (2014) experimental model

3. Analysis of the Results

3.1. Heat Transfer Analysis in Steel and Concrete Sections

As stated before, the first aim of this study is to analyze heat transfer in steel and concrete sections by considering cracking effects in concrete. For this end all the structural sections of Table 1 were put under thermal analysis. At first, two steel and concrete sections with similar size were exposed to fire load based on Euro Code heat transfer analysis. In this part of the study, a 45×45 concrete box section, and a 45×2 steel box section were exposed to fire load, which was presented by ISO 834 standard for each of the dimensions. Fire load was applied on the sections for 2 hours (7200 sec) and heat transfer was analyzed in two sections. Different boundary conditions were considered for beam and column sections. For the beam element it was assumed that the fire load is entered only under the element The analysis results are indicated in Figure 11. Based on this figure, heat transfer in steel section is higher than concrete section. Estimation of thermal intervals in the depth of sections indicates that applying heat on the lower dimension of the section will transfer the heat to upper dimensions. However, this transfer is higher in steel sections in comparison with concrete sections. Lower specific heat and higher thermal conductivity coefficient of steel are the reasons for higher heat transfer of steel sections in comparison with concrete sections.

Figure 12 indicates temperature-time curves of lower half (exposed to fire) of the section. It is a function which includes the ratio of depth (D) to height (H). The results

of heat transfer analysis indicate that both concrete and steel sections are located in the lowest section (D/H = 0.5) of temperature-time curve which has been presented by ISO standard. It indicates that heat is dependent on fire load in those sections which are exposed to fire. By getting away from the section which is exposed to fire in steel sections (D/H = 0.4), the trend of temperature rise is similar to the trend of fire-exposed section. However, this temperature is lower than fire temperature. This trend is also observable in concrete section, but maximum temperature in this section is lower than the steel section. This trend exists for the ratio of D/H = 0.3. However, for D/H = 0.1 and D/H = 0.2 ratios, temperature due to fire is so low in concrete section. Therefore, in analyzing the depth of D/H = 0.2, temperature is 140 $^{\circ}$C, and in the depth of D/H = 0.1, temperature is 80 $^{\circ}$C. However, in concrete section, heat transfer trend is in the form of temperature rise in fire-exposed dimension. Maximum temperature in steel sections with D/H = 0.2 and D/H = 0.1 ratios are 530 $^{\circ}$C and 450 $^{\circ}$C, respectively.

The effect of cracking and spalling caused by a seismic load on heat transfer analysis in reinforced concrete sections is considered, based on wen et al. (2015) and Behnam and ronagh (2013). In any seismic intensity, the damage index has been used to determine cracking and spalling (Wen et al., 2020).

In the following, the effects of cracking on heat transfer of concrete sections is studied. Since concrete sections are vulnerable against seismic loads, some cracks may appear on them. Width and depth of the crack are different in various

damaged levels. For example, according to the Damage Class Definition, damage class II refers to those cracks with a width range from 0.2 to 1 mm in concrete sections. This trend will reach to more than 2 mm in class IV. In this study, two II and IV classes of cracks were selected as cracking criterions in order to estimate their effects on heat transfer process of concrete sections. Figure 13 indicates heat transfer of 40×40 concrete section with two II and IV cracks under fire load of ISO 834. In class II, some cracks with a width of 0.5 mm and low depth were selected. In class IV, some other cracks were selected in addition to the cracks of class II with a width of more than 3 mm and more depth for the cover of concrete sections. According to Figure 13, cracks cause the depths to expose directly to the environmental heat, and therefore, increase heat transfer.
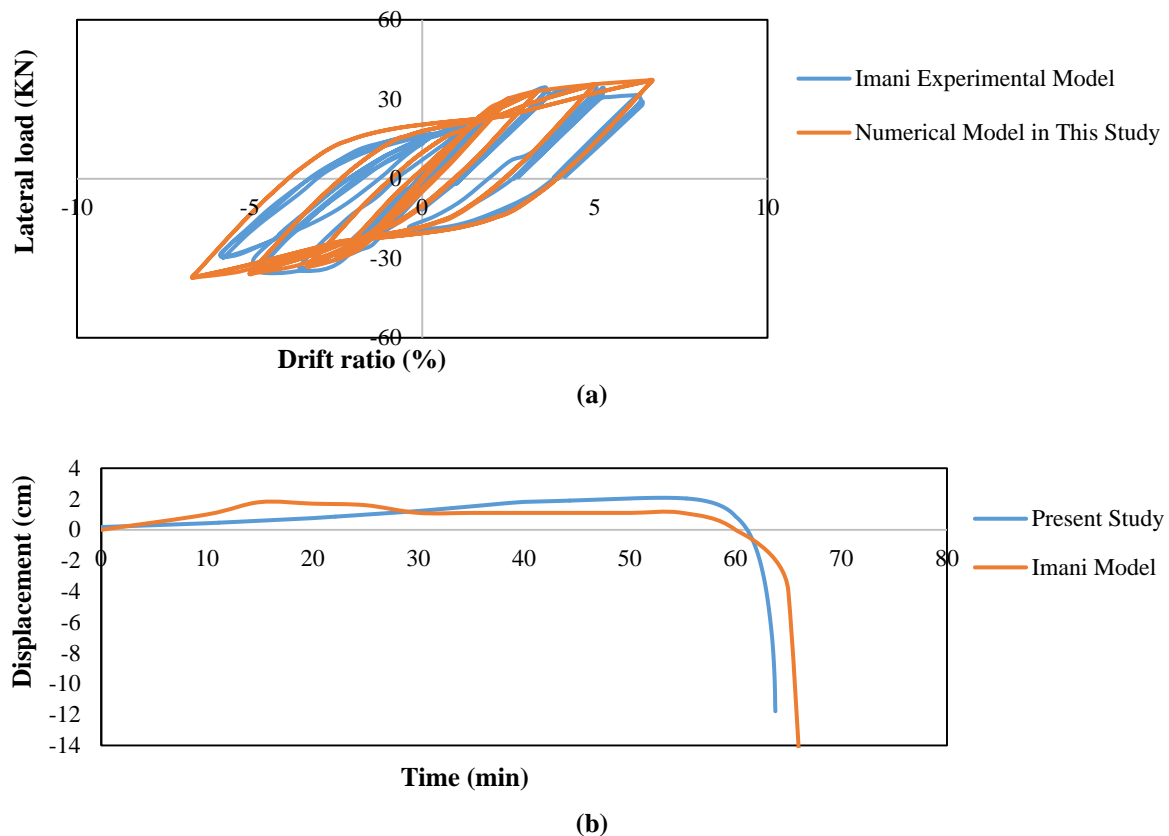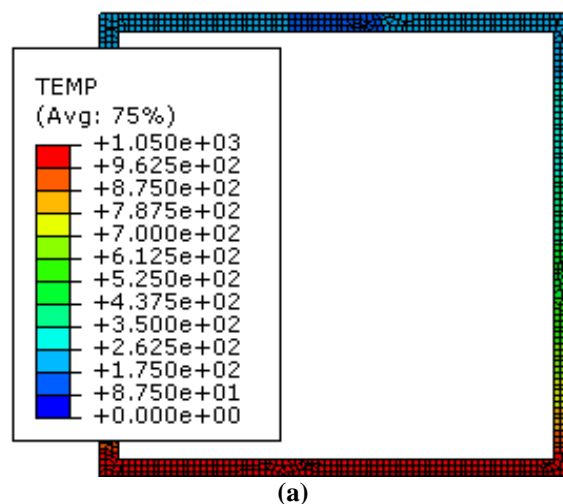

(a)

(b)

Fig. 10. Modeling results in this study and Imani et al. (2014) experimental model: a) Cyclic loading and; b) Post cyclic loading
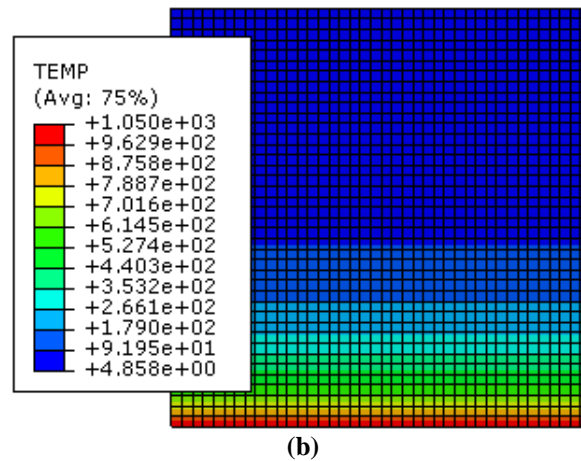

(a)

(b)

Fig. 11. Heat transfer in: a) Steel and; b) concrete sections under ISO 834 fire load
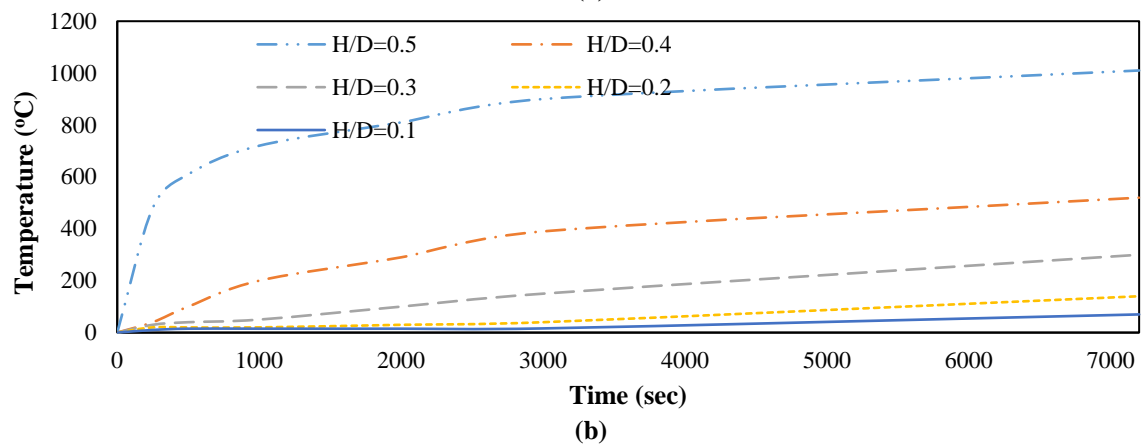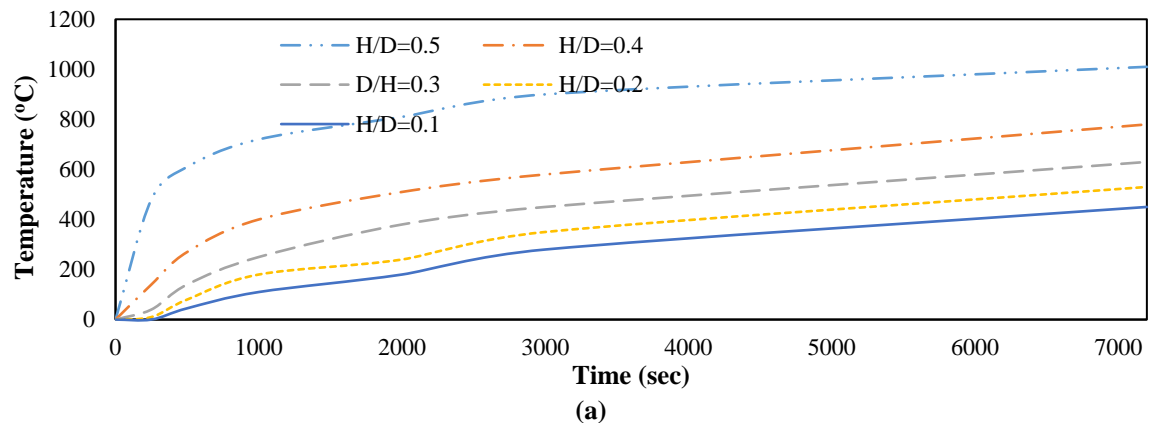

(a)

(b)

Fig. 12. Temperature-time curves in the depth of: a) Steel and; b) Concrete sections under ISO fire load

Temperature in cracks is a function of environmental heat and fire. Figure 14 indicates temperature-time curves for different values of D/H. According to this figure, low depth cracks (class II) on the section have weaker effects on heat transfer. The curves of Figures 12b and 13b are similar. They indicated that capillary cracks have no effects on heat transfer of the sections. Wider and deeper cracks accelerate heat transfer process of the section. The most effects can be observed in

D/H = 0.3 and D/H = 0.4 depths.

In the following, heat transfer in all sections of Table 1 and all the fire loads are presented in section 2.4. The results of heat transfer analysis are indicated in Figure 15 by mean of average area, standard deviation, and mean minus standard deviation in steel and concrete sections with and without cracks. These results indicate that maximum mean of temperature are higher in the depth of steel section in comparison with cracked or crack-less

concrete section. Moreover, they indicate that the more get away from fire-exposed side, the lower the standard deviation and mean values will be. The results of experiments indicate that high width and high depth cracks will increase mean of temperature in various depths of the section.
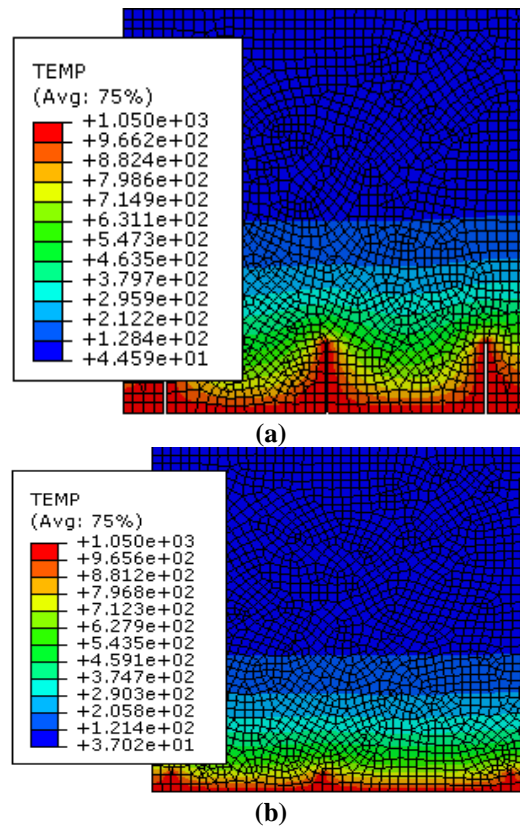

(a)

(b)

Fig. 13. Heat transfer in concrete section: a) Section with wide and deep cracks and; b) Sections with capillary cracks, under ISO 834 fire load
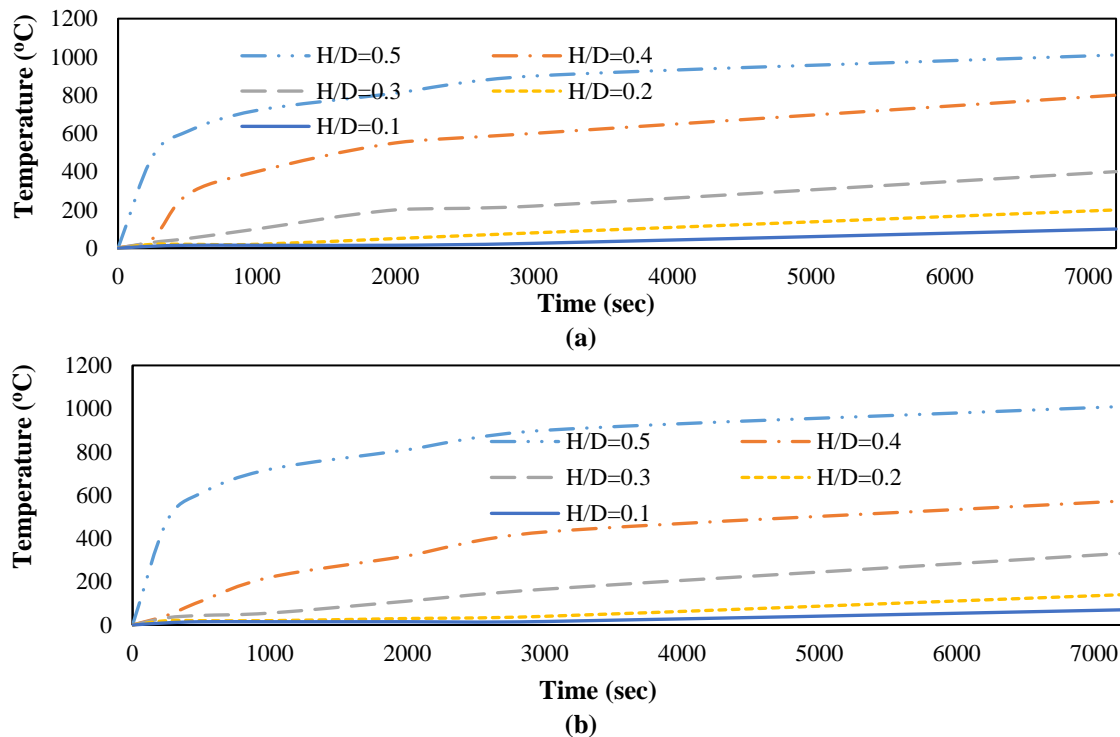

(a)

(b)

Fig. 14. Temperature-time curves in depth of concrete section with ISO 834 fire load: a) Section with wide and deep cracks and; b) Sections with capillary cracks
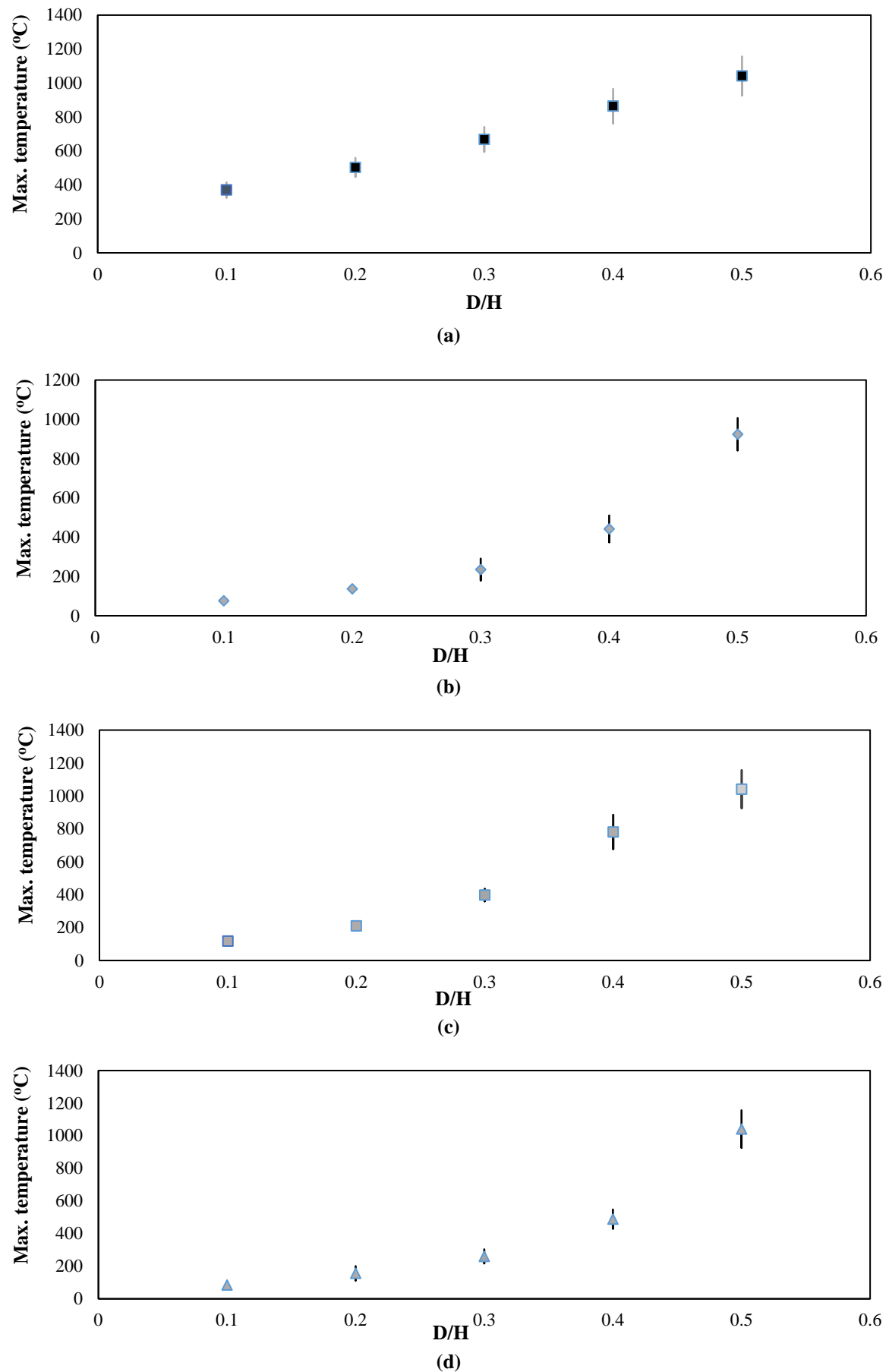
Fig. 15. Max. temperature changes in depth of: a) Steel; b) Crack-less concrete; c) Cracked concrete and; d) capillary cracked concrete sections

3.2. Failure Criterion

There are various criterions to evaluate the response and the strength of structures against thermal loads. Middle span vertical displacement is one of these (Ali and Hasan, 2020).

The time of a sudden increase in the vertical displacement of the middle span of the beam is considered as the failure criterion of the structure under PEF loads. The moment that the middle span vertical displacement increases suddenly, has been considered as the failure point of frames. For example, Figure 16 shows the middle span vertical displacement of 6th story under fire and PEF load after Kocaeli record. Steel frame has been failed in Figure 16, at 1959th second under fire and at 1915th second under PEF loads. Also, middle span vertical displacement in reinforced concrete frame under fire load was very few during 120 minutes. This indicates that this frame has not been failed due to fire load. Middle span vertical displacement in reinforced concrete frame due to PEF load of Kocaeli earthquake has increased suddenly at 2466th second. It shows that the failure has been occurred.

3.3. Evaluation of Frame Response in Fire Loading

After heat transfer analysis and extraction of temperature-time curves from the depth of sections, durability of frames in fire scenario was assessed. Fire load was applied on middle spans of first, third, and sixth stories and their durability was extracted. Based on the results, ISO 834 fire load was applied on the concrete frames for 120 minutes. They preserved their stability and did not damaged. However, steel frames which were put under fire load for 32 minutes in the first story, for 29 minutes in the third story, and for 27 minutes in the sixth story, were widely damaged.
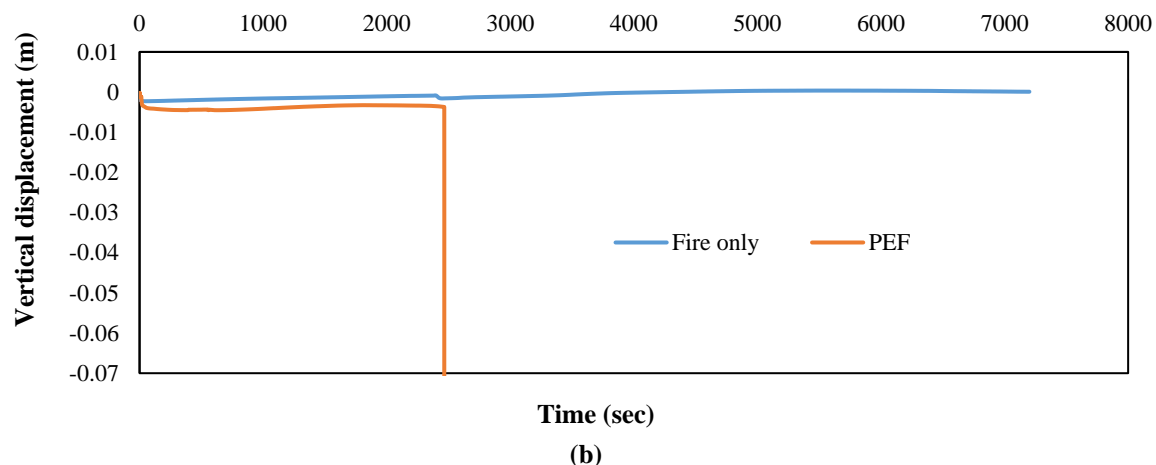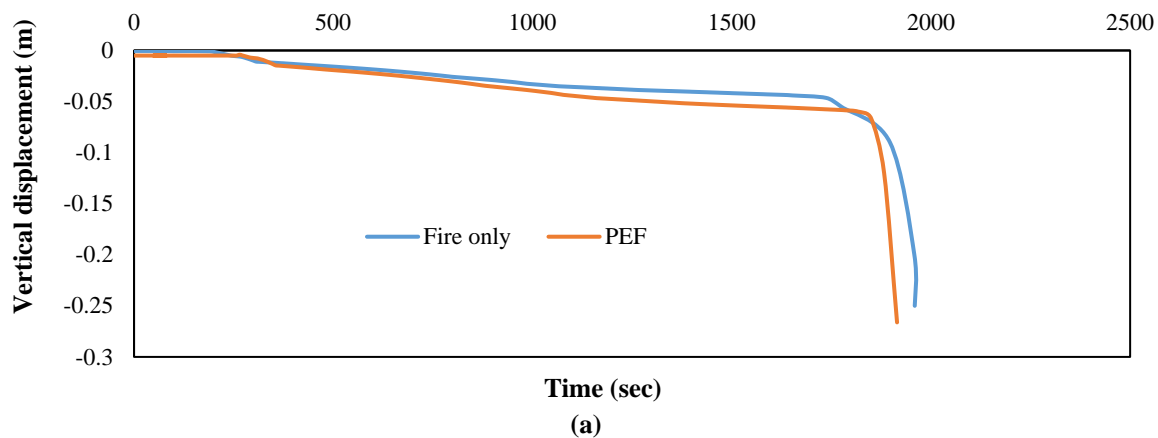

(a)

(b)

Fig. 16. Vertical displacement at middel span under fire and PEF loading: a) Steel moment frame and; b) RC moment frame

Figure 17 indicates the results of other fire loads for steel and reinforced concrete frames in different stories. According to this figure, reinforced concrete frame in all the loading scenarios remained stable and no failure occurred in their fire span. Steel frames remained stable under Q100 and Q300 fire loads for two hours. However, more failure occurred in their fire spans under higher fire loads. If fire load increases, the duration of stability decreases in steel frames. It should be noted that damage time in different stories are near to each other. The least failure time in steel frames was observed in Q1000 fire load and failure had been accrued after 21 minutes. The results indicate that heat transfer is slow in reinforced concrete frames. Therefore, their strength decrease due to fire is higher than steel frames. Heat transfer in sections of steel frames are faster than reinforced concrete frames. Temperature rise in the depth of sections decreases their strength and leads to the instability of structure.

3.4. Evaluation of Frame's Behavior in PEF Loading

In the rest of the research process, the behavior of reinforced concrete and steel frames in PEF loadings are assessed. For this end, one of the seismic load combination in Table 4 was applied on each structure. Their responses were assessed and strength reduction in fire spans was estimated. Tables 5 and 6 indicate these responses for seismic loads. The response of seismic load is presented by the ratio of story acceleration to the basic spectral acceleration with 5% damping ($Sa_{5\%}$). Moreover, drift ratios of reinforced concrete and steel frames are shown in Tables 5 and 6. Seismic load responses for two Sa and drift ratio criterions indicate that the selected seismic load distributed these two indicators efficiently. Sa of steel frames ranges from 0.31 to 2. Drift values was expanded from 0.002 to 0.036. These values in reinforced concrete frames were 0.28 to 2.04 for Sa, and 0.002 to 0.037 for drift ratio.
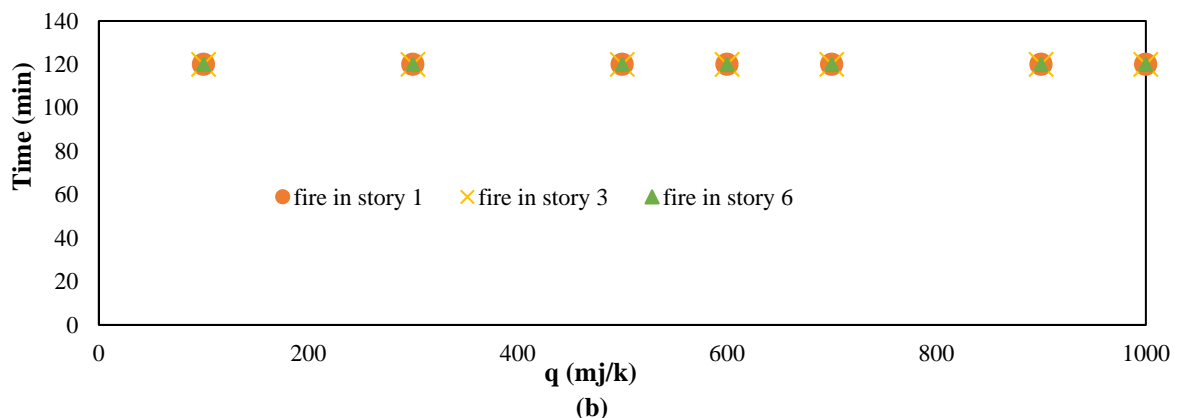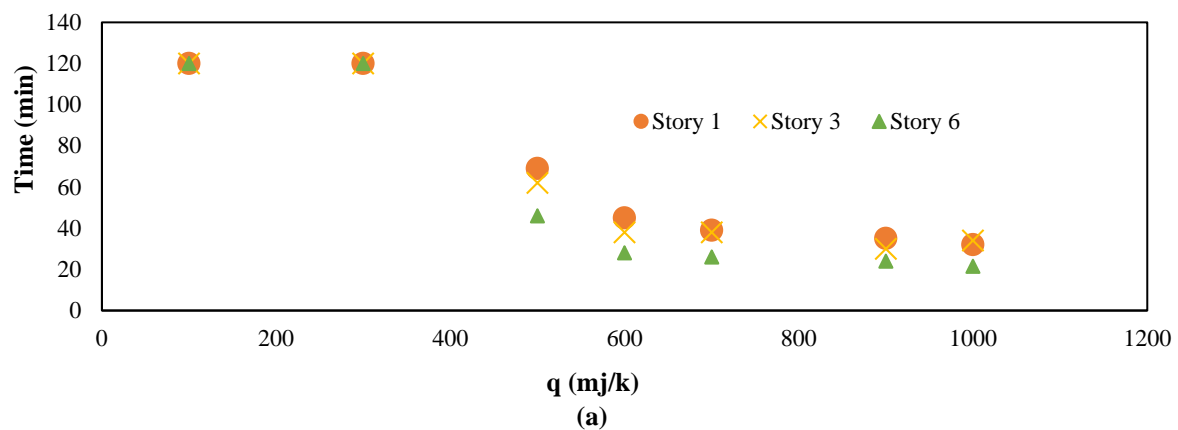

Fig. 17. Durability of frames in fire scenarios: a) Steel and; b) Reinforced concrete frames

Table 5. The response of steel frame to seismic loads in the specified span

Earthquake	Sa (5%)			Drift ratio		
	Story 1	Story 3	Story 6	Story 1	Story 3	Story 6
Niigata	0.53	1.38	1.51	0.006	0.0153	0.0176
Kobe	0.466	1.2	1.5	0.004	0.0128	0.0168
Loma Prieta	0.4	1.06	1.99	0.0028	0.0068	0.014
Northridge	0.4	1.37	1.35	0.0034	0.0121	0.026
San Fernado	0.7	1.36	1.36	0.0034	0.012	0.027
Bam	0.51	1.01	2	0.0073	0.029	0.028
Hector Mine	0.55	1.78	1.76	0.0046	0.0133	0.02
Kocaeli	0.46	1.57	1.69	0.0048	0.019	0.034
Landers	0.31	1.05	1.33	0.012	0.03	0.036
Manjil	0.67	1.7	1.27	0.003	0.0046	0.0104

Table 6. The response of reinforced concrete frame to seismic loads in the specified span

	Sa (5%)			Drift ratio		
	Story 1	Story 3	Story 6	Story 1	Story 3	Story 6
Niigata	0.71	1.8	1.78	0.0067	0.0106	0.0227
Kobe	0.51	1.21	1.5	0.008	0.0124	0.021
Loma Prieta	0.446	1.05	2.04	0.003	0.00643	0.0183
Northridge	0.48	1.53	1.37	0.006	0.0094	0.0328
San Fernado	0.51	1.5	1.4	0.006	0.0093	0.0329
Bam	0.57	1.37	2.3	0.0101	0.0168	0.037
Hector Mine	0.61	1.98	1.75	0.00653	0.0104	0.0283
Kocaeli	0.54	1.53	2	0.0094	0.015	0.037
Landers	0.28	0.8	1.33	0.013	0.019	0.03
Manjil	0.69	1.6	1.43	0.002	0.0043	0.0091

After nonlinear dynamic analysis and estimation of seismic parameters, strength decrease was estimated by Altootash's recommendations for damaged spans (Lowes and Altoontash, 2003). After modification of strength values for each element, fire load was applied on the specified span after each seismic load. Then, responses of two selected frames were extracted according to their durability. Moreover, the cracks and their effects on the heat transfer of reinforced concrete frames were analyzed for fire load modeling. At first, durability of reinforced concrete and steel frames were estimated by temperature-time curves of ISO 834 for different seismic loads and fire places.

18 presents durability of reinforced concrete and steel frames for ISO 834 scenario which were exposed to different earthquakes. Two presented curves of figure 18 shows significant differences between the behavior of reinforced concrete and steel frames against PEF scenarios. The first difference is in their durability.

Durability of steel frames in PEF scenarios ranges from 32 to 26 minutes, while this parameter ranges from 120 to 42 minutes in reinforced concrete frames.

This difference indicates that durability of reinforced concrete frames is higher than steel ones in PEF scenarios. The second difference is in the behavior of reinforced concrete and steel frames according to the ratio of durability changes to drift. Durability of reinforced concrete frame, which is exposed to ISO 834 fire load, is 120 minutes in 0.012 drift.

By increasing the drift of different stories, durability decreases and the structures experience damages in their PEF region. In a nearly 0.02 drift, durability varies for third and sixth stories. Since in reinforced concrete frames , the third story have larger dimensions in comparison with the sixth story, and heat transfer from fire dimension to the core occurs more slowly, this fire region has higher durability in comparison with the sixth story. According to the increase of drift values in the sixth story, cracking and durability reduction of this story is lower than the others. Despite of reinforced concrete frame, durability of steel frames of three stories have no

significant differences in PEF loading. In fact, the results indicated that sensitivity of steel frame to earthquake is not significant in PEF loading.

Another behavioral difference of reinforced concrete and steel frames is their failure mode in fire. It is observed that failure mode of steel frames is ductile. So

that before total failure of steel frame, large deformations occur in the frame. This trend is in the form of brittle failure in reinforced concrete frames. They fail without any significant deformation. Figure 19 shows some examples of deformation in reinforced concrete and steel frames in sixth story fire.
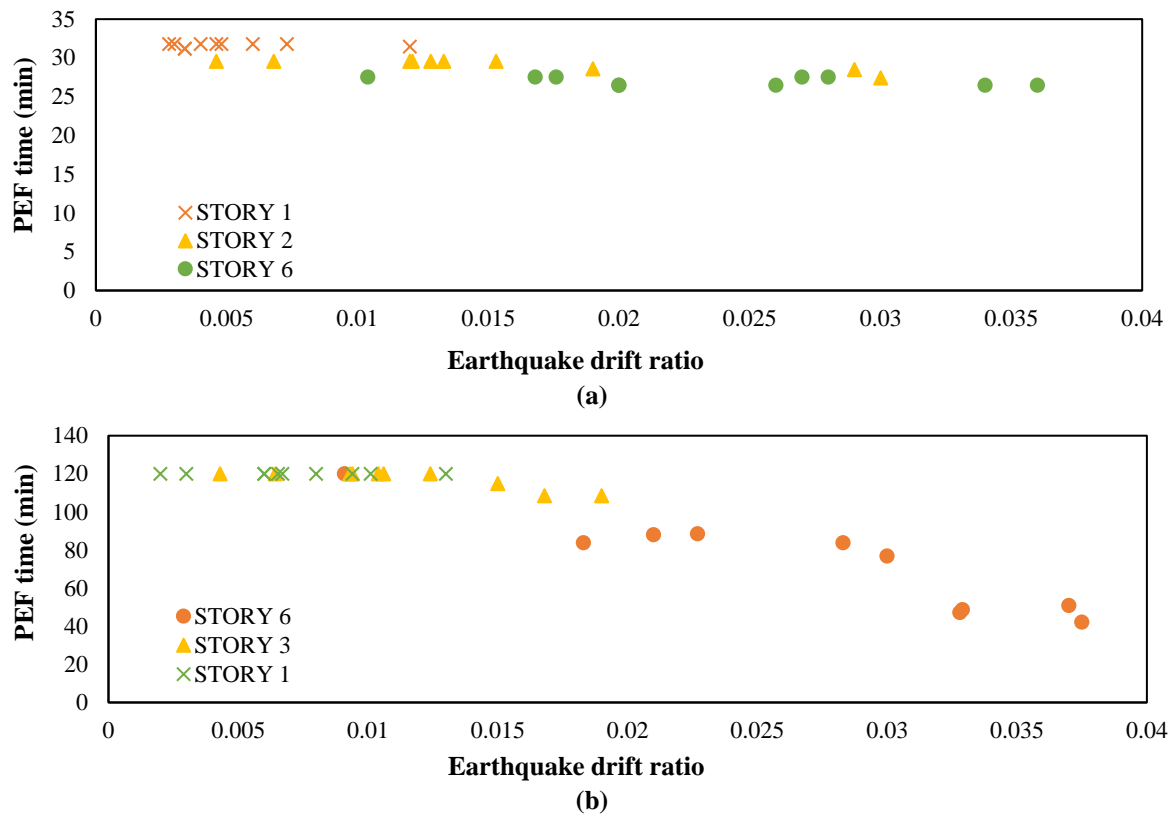

(a)

(b)

Fig. 18. Durability values of frames in ISO 834 PEF fire scenarios: a) Steel and; b) Reinforced concrete frames

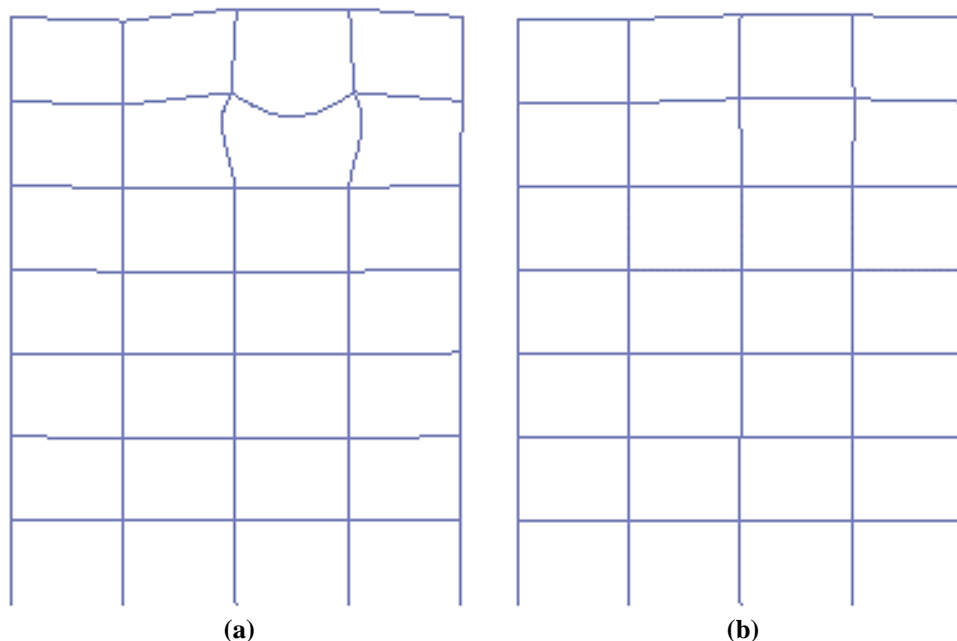   **(a)**   **(b)**

Fig. 19. Frame deformation in PEF scenarios of a) steel and; b) reinforced concrete frames

In the following, durability of reinforced concrete and steel frames in PEF's are surveyed. According to the Figure 20b, durability of reinforced concrete frame in the first story is 120 minutes in each PEF. Since drift values of this story are low, and its strength reduction and cracking effects are not significant, all the analysis of this story indicate 120 minutes durability for reinforced concrete frames.

Figure 20a indicates the results of the durability for the first story of steel frames in earthquake and different fire loads of PEF scenarios. According to this figure, maximum durability of Q100 and Q300 fire loads are estimated to be 120 minutes (maximum analysis duration). For greater fire loads, durability of the frame decreases. This decrease is observable in the form of horizontal lines. These horizontal lines represent that different response values against seismic loads (drift) have no significant effect on durability of the frame. This effect can only be several minutes. Moreover, durability in Q700, Q900, and Q1000 are so close to each other.

Figure 20d indicates temperature-time curve for reinforced concrete frames against PEF at the third story. As it is obvious in the figure, applying Q700, Q900, and Q1000 loads will decrease durability of the frames against fire loads. This decrease is observable in maximum drifts of 0.016.

Figure 20c shows durability of steel frames in PEF scenarios. In this scenarios, fire is in the middle frame of the third story. Similar to the fire scenario of the first story in steel frame, each fire load is in the form of horizontal lines. It indicates that the effects of seismic loads on durability of steel frames is not significant. This trend is observable in Figure 20e which includes durability of the steel frames against PEF's of the sixth story.

Figure 20f indicates durability of reinforced concrete frame of the sixth story against fire. Despite of lower stories, distribution of the durability time at this fire position is significantly more. In this fire position, durability of the reinforced concrete frame decreases with an increase in fire load and drift. This decrease, in the worst case, is two times more than durability decrease of steel frames.
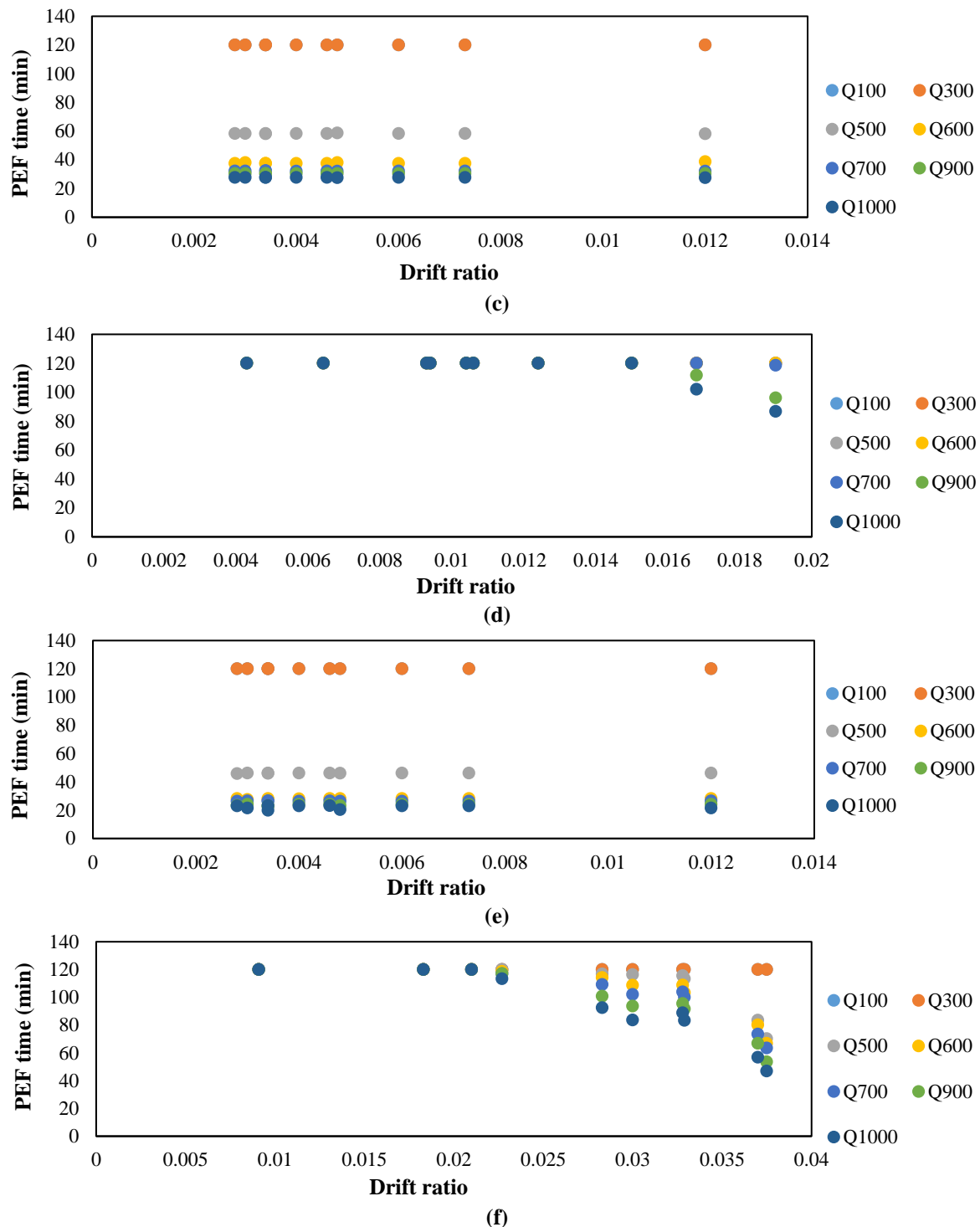

(a)

(b)

(c)

(d)

(e)

(f)
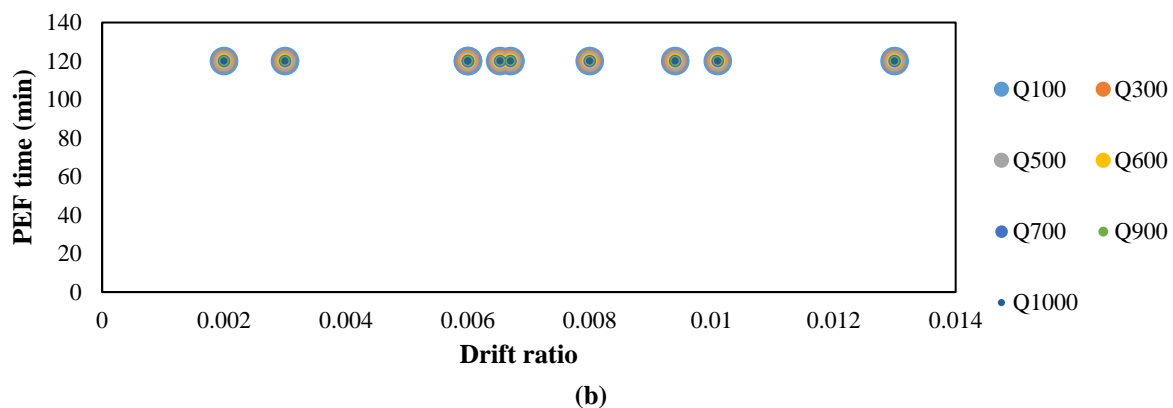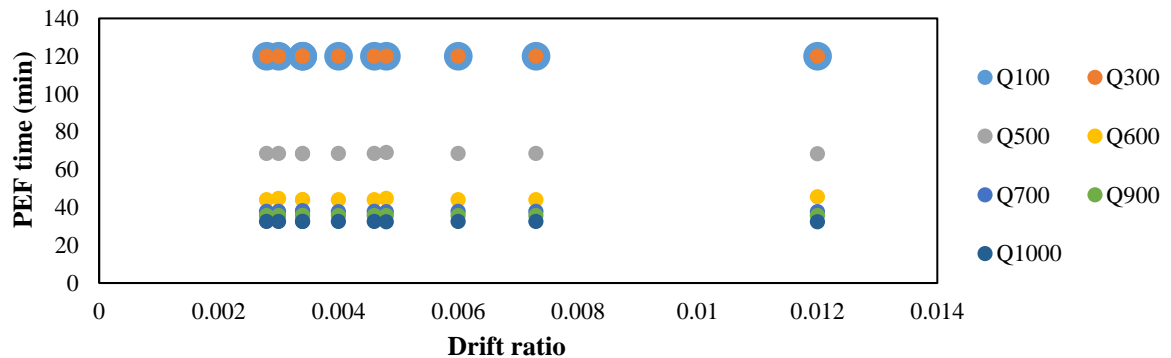
Fig. 20. Durability time of the reinforced concrete and steel frames in PEF scenarios: a) The first story of the steel frame; b) The first story of reinforced concrete frame; c) The third story of the steel frame; d) The third story of the reinforced concrete frame; e) The sixth story of the steel frame and; f) The sixth story of the reinforced concrete frame

In the following, after analyzing the effects of spectral acceleration ($Sa_{5\%}$) on durability of frames in PEF scenarios, durability diagram of steel and reinforced concrete frames of the sixth story are indicated in Figure 21 with different drift values. Sa has no significant effect on durability of steel frames. However, each Sa, especially small Sa, has a significant effect on durability of reinforced concrete frames. Drift criterion can be a suitable measurement to analyze the effects of seismic loads on durability during PEF scenarios.
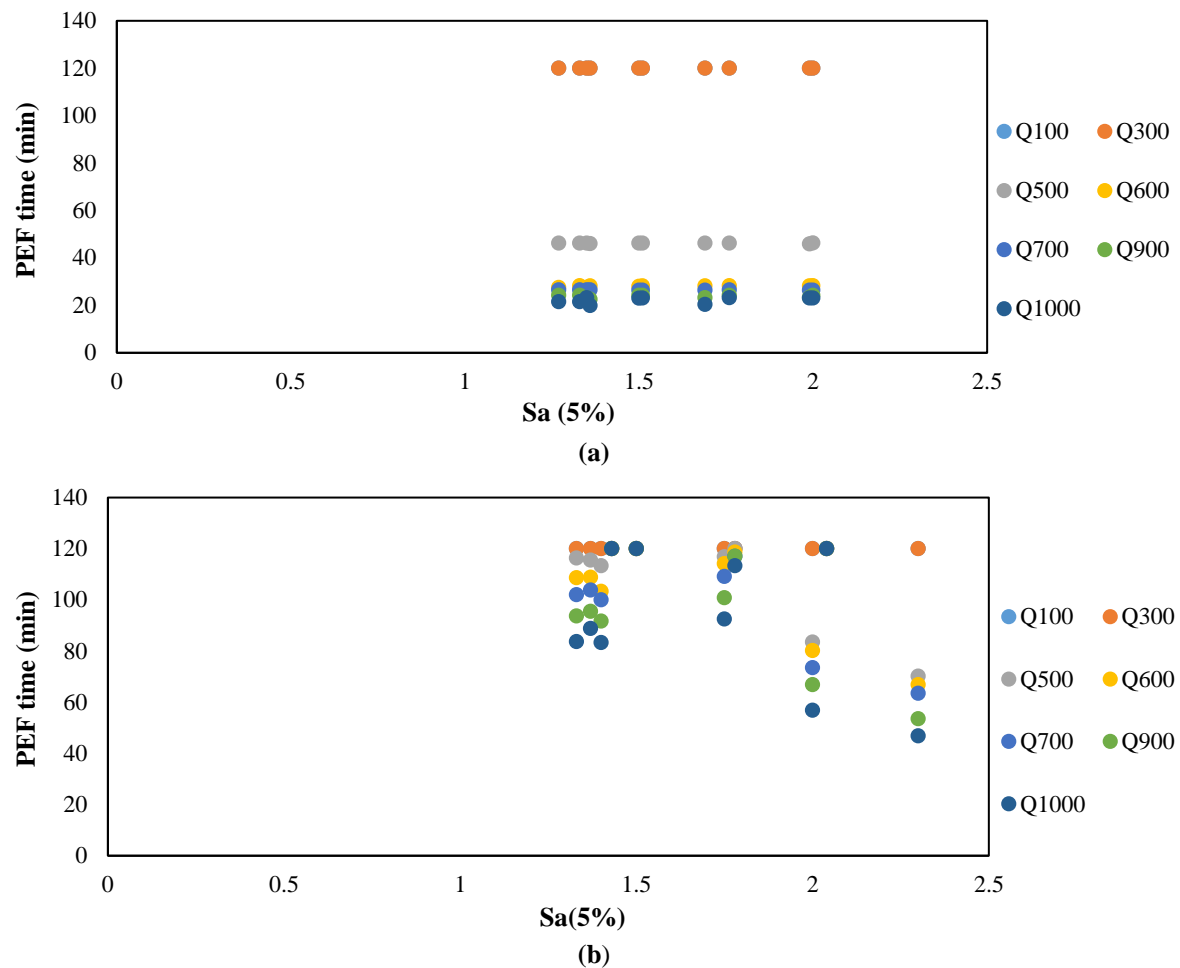
Fig. 21. Durability of frames in the sixth floor in PEF's: a) Steel and; b) Reinforced concrete frame

4. Summary and Results

The aim of this study was to evaluate durability of reinforced concrete and steel frames. For this end, two 7-story frames were designed based on Iranian standards. Then, different sections of these frames were exposed to thermal loads in order to analyze their heat transfer. Therefore, heat transfer of box and I-shaped steel sections, and square-shaped reinforced concrete sections were examined. In the next step, the effects of cracks on heat transfer of concrete sections were studied. Then, thermal analysis were done on steel and reinforced concrete frames for 8 fire loads in three locations and their durability were estimated. Then, durability of the frames in different PEF's was evaluated. In this study, the following points are resulted:

- The analysis of heat transfer in steel and concrete sections indicated that heat transfer trend is fast in steel sections. This trend is also observable in cracked concrete sections.

- Capillary cracks have no significant effect on the heat transfer of concrete sections. However, deep cracks will speed up the heat transfer procedure.

- In all the fire scenarios under each kind of the fire load, reinforced concrete frames remain stable during 2 hours of the analysis. However, some failure will be observable in steel frames after this duration.

- Durability of the reinforced concrete frames is sensitive to input seismic loads. However, steel frames indicated no significant sensitivity toward seismic loads in PEF scenarios. Durability of steel frames is not different in fire and PEF scenarios.

- Durability of reinforced concrete frames, despite the steel frames, is a function of

structural response to seismic load. If maximum drift in earthquake scenario be more than 0.015, durability of reinforced concrete frames will decrease in PEF scenario. By increasing the maximum drift, durability of the reinforced concrete frame will decrease further. However, durability of steel frames is not a function of input load. It has no significant difference with the durability in fire scenario.

- Cracks in reinforced concrete sections and their effects on heat transfer, along with reduction in strength of concrete elements due to seismic loads decrease durability in PEF scenarios with maximum drift (exposed to earthquake) in comparison with PEF scenarios. However, in steel frames, fast heat transfer and strength reduction create further instabilities and failures. Strength reduction in connecting points of beams to columns in steel frames has no effects on instability of these frames in PEF's. The determinant factor is the amount of fire load and heat transfer mode in steel sections.

- By comparing the relationship between maximum drift and Sa in PEF scenario with durability of reinforced concrete frames, it is indicated that increase of both drift and Sa parameters will decrease durability. However, drift ratio represents a better trend in decreasing of durability for this frame.

5. Acknowledgments

6. References

Ali, A.S. and Hasan, T.M. (2020). "Flexural behavior of fiber reinforced self-compacting rubberized concrete beams", *Journal of Engineering*, 26(2), 111-128.

Barkavi, T. and Naratarajan, C. (2019). "Processing digital image for measurement of crack dimensions in concrete", *Civil Engineering Infrastructures Journal*, 52(1), 11-22.

Elhami Khorasani, N. and Garlock, M.E. (2017). "Overview of fire following earthquake: Historical events and community responses", *International Journal of Disaster Resilience in the Built Environment,* 8(2), 158-174.

Eskandari, M., Rahimian, M., Mahmoodi, A. and Ardeshir, A. (2013). "Analytical solution for two-dimensional coupled Thermo-elasto-dynamics in a cylinder", *Civil Engineering Infrastructures Journal*, 46(2), 107-123.

Felicetti, R. and Gambarova, G. (1996). "Residual mechanical properties of high-strength concretes subjected to high-temperature cycles", *4th International Symposium on Utilization of High-Strength/High-Prformance Concrete*, Paris, pp. 579-588.

Imani, R. and Mosqueda, G. (2014). "Experimental study on post-earthquake fire resistance of ductile concrete-filled double-skin tube columns", *Journal of Structural Engineering,* 141(8), 04014192.

Kadir, A. and Zhang, J. (2012). "Modeling of an earthquake damaged RC frame subjected to fire", *Proceedings of 7th International Conference on Structures in Fire*, U.K., pp. 479-488.

Keller, W.J. and Pessiki, S. (2012). "Effect of earthquake-induced damage to spray-applied fire-resistive insulation on the response of steel moment-frame beam-column connections during fire exposure", *Journal of Fire Protection Engineering,* 22(4), 271-299.

Keller, W.J. and Pessiki, S. (2015). "Effect of earthquake-induced damage on the sidesway response of steel moment-frame buildings during fire exposure", *Earthquake Spectra,* 31(1), 273-292.

Khorasani, N.E. and Garlock, M. (2014). "Fire load: Survey data, recent standards, and probabilistic models for office buildings", *Engineering Structures,* 58(2), 152-165.

Kotsovinos, P. and Usmani, A. (2013). "The World Trade Center 9/11 disaster and progressive collapse of tall buildings", *Fire Technology,* 49(3), 741-765.

Lee, S.W. and Davidson, R.A. (2010). "Physics-based simulation model of post-earthquake fire spread", *Journal of Earthquake Engineering*, 14(5), 670-687.

Liu, G.-R. and Song, Y.P. (2010). "Post-fire cyclic behavior of reinforced concrete shear walls", *Journal of Central South University of Technology,* 17(5), 1103-1108.

Lowes, L.N. and Altoontash, A. (2003). "Modeling reinforced-concrete beam-column joints subjected to cyclic loading", *Journal of Structural Engineering*, 129(12), 1686-1697.

Memari, M. and Mahmoud, H. (2014). "Post-earthquake fire performance of moment resisting

frames with reduced beam section connections", *Journal of Constructional Steel Research,* 103(2), 215-229.

Moradi, M., Tavakoli, H.R. and Abdolahzade, G. (2019). "Sensitivity analysis of the failure time of reinforcement concrete frame under postearthquake fire loading", *Structural Concrete,* 21(1), 625-641.

Moradi, M. and Tavakoli, H.R. (2019). "Probabilistic assessment of failure time in steel frame subjected to fire load under progressive collapses scenario", *Engineering Failure Analysis,* 102(1), 136-147.

Natesh, P.S. and Agarwal, A. (2020). "Numerical Modelling of continuous composite beam under fire loading", *Advances in Structural Engineering*, 74(1), 73-88.

Nishino, T. and Tanaka, T. (2012). "An evaluation method for the urban post-earthquake fire risk considering multiple scenarios of fire spread and evacuation", *Fire Safety Journal,* 54(2), 167-180.

Schar, Y.M. and Dancy, A.N. (2020). " Assessment of reinforced concrete slabs post-fire performance", *Fire Safety Journal*, 111(1), 102932.

Sharma, U.K. and Bhargava, P. (2012). "Full-scale testing of a damaged reinforced concrete frame in fire", *Structures and Buildings,* 165(7), 335-346.

Tan, Q.H., Garden, L., Han, H. and Song, T. (2020). "Performance of concrete-filled stainless steel tubular (CFSST) columns after exposure to fire", *Thin-Walled Structures*, 146(3), 106629.

Tavakoli, H. and Afrapoli, M.M. (2018). "Robustness analysis of steel structures with various lateral load resisting systems under the seismic progressive collapse", *Engineering Failure Analysis,* 83(5), 88-101.

Tavakoli, H.R. and Kiakojuri, F. (2015). "Threat-independent column removal and fire-induced progressive collapse: Numerical study and comparison", *Civil Engineering Infrastructures Journal*, 48(1), 121-131.

Usmani, A. and Zhang, J. (2012). "Using opensees for structures in fire", *Journal of Structural Fire Engineering,* 3(1), 57-70.

Wen, B., Zhang, L., Wu, B. and Niu, D. (2020). "High-temperature performance of damaged reinforced concrete columns under post-earthquake fires", *Structure and Infrastructure*, 10(1), 1-5.

Wong, M. and Ghojel, J.I. (2003). "Sensitivity analysis of heat transfer formulations for insulated structural steel components", *Fire Safety Journal,* 38(2), 187-201.

Zolfaghari, M. and Peyghaleh, E. (2009). "Fire following earthquake, intra-structure ignition modeling", *Journal of Fire Sciences,* 27(1), 45-79.